Magnetic Properties of 3-(4-R-Phenyl)-1,5-diphenyl-6-oxo- and -thioxoverdazyl Radical Crystals (R = OCH$_3$, CH$_3$, CN, and NO$_2$)

Kazuo Mukai,[†,]* Masaaki Nuwa,[†] Kentaro Suzuki,[†] Shin-ichi Nagaoka,[†] Norio Achiwa,[‡] and Javad B. Jamali[‡]

Department of Chemistry, Faculty of Science, Ehime University, Matsuyama 790-77, and Department of Physics, Faculty of Science, Kyushu University, Hakozaki, Fukuoka 812, Japan

Magnetic susceptibilities of 8 kinds of 3-(4-R-phenyl)-1,5-diphenyl-6-oxo- and -thioxoverdazyl radical crystals (*p*-MDpOV (R = OCH$_3$), *p*-MeDpOV (R = CH$_3$), *p*-CyDpOV (R = CN), *p*-NDpOV (R = NO$_2$), *p*-MDpTV (R = OCH$_3$), *p*-MeDpTV (R = CH$_3$), *p*-CyDpTV (R = CN), and *p*-NDpTV (R = NO$_2$)) were measured between 4.2 and 300 K. The susceptibilities of *p*-MDpOV, *p*-CyDpOV, and *p*-MDpTV can be well explained by a one-dimensional (1D) antiferromagnetic (AFM) Heisenberg linear chain model with exchange interaction of $2 J/k = -27.3$, -27.3, and -10.9 K, respectively. The susceptibility of *p*-MeDpTV can be interpreted in terms of a 1D AFM Heisenberg alternating chain model with $2 J_1/k = -92.0$ K (alternation parameter $\alpha = J_2/J_1 = 0.7$). On the other hand, the susceptibilities of *p*-MeDpOV, *p*-NDpOV, and *p*-CyDpTV follow the Curie−Weiss law with positive Weiss constants of $+2.5$, $+1.5$, and $+2.9$ K, respectively, and the exchange interactions $2 J/k$ were estimated to be $+7.0$, $+5.0$, and $+7.0$ K, assuming the one-dimensionality for these radical crystals. The susceptibility of *p*-NDpTV follows the Curie−Weiss law with a negative Weiss constant of -0.9 K. Ab initio molecular orbital (MO) calculation was performed for five kinds of 6-oxoverdazyl radicals to clear the origin of the intermolecular ferromagnetic exchange interaction that is observed with high probability for these verdazyl radicals. A very strong spin polarization effect has been found, which is advantageous to the intermolecular ferromagnetic interaction.

Introduction

The study of magnetic properties of organic radical crystals has attracted much attention since the finding of the first organic ferromagnet, *p*-nitrophenyl nitronyl nitroxide (β-phase; Curie temperature (T_c) = 0.60 K), in 1991.[1−3] Although 18 kinds of organic ferromagnets have been found since 1991, the examples are almost limited to nitroxide and nitronyl nitroxide radicals.[4−15] Furthermore, the highest T_c (1.48 K) observed for a nitroxide biradical is very low compared with those of transition metals (T_c = 1043 K for Fe, T_c = 1388 K for Co, and T_c = 627 K for Ni).[4,5] Therefore, the search for new kinds of organic ferromagnets with a high T_c remains a matter of high interest.

Recently, the synthesis of a new type of 1,5-diphenyl-6-oxo- and -thioxoverdazyl radicals has been performed by Neugebauer et al.[16] These verdazyl radicals show a high chemical and thermal stability and can be isolated as solvent-free pure radicals in crystalline states. Kremer et al.[17] found that the 1,3,5-triphenyl-6-oxoverdazyl (TOV) radical shows the property of weak ferromagnetism below T_N = 4.9 K. To our knowledge, this is the second example of weak ferromagnet found for a genuine organic radical crystal. We studied the magnetic property of four kinds of this type of verdazyl radicals[18] and found that 3-(4-chlorophenyl)-1,5-diphenyl-6-oxoverdazyl (*p*-CDpOV) is a new ferromagnet with a T_c of 0.21 K.[14] *p*-CDpOV behaves as a quasi-one-dimensional (1D) Heisenberg ferromagnet with the intrachain exchange interaction of $2 J/k = +11$ K

above the transition temperature T_c. The interchain exchange interaction zJ'/k was estimated to be $+0.03$ K, where z is the number of interchain bonds per spin, showing high one-dimensionality in *p*-CDpOV.

In the present work, we prepared eight kinds of 3-(4-R-substituted-phenyl)-1,5-diphenyl-6-oxo- and -thioxoverdazyl radicals (R = OCH$_3$, CH$_3$, CN, and NO$_2$; see Figure 1), and studied the magnetic property of these radical crystals. Ferromagnetic (FM) intermolecular exchange interactions were observed with high probability for these verdazyl radical crystals, and thus the ab initio MO calculations were performed for 3-(4-R-phenyl)-1,5-diphenyl-6-oxoverdazyl radicals (R = H, OCH$_3$, CH$_3$, CN, and NO$_2$) to ascertain whether the verdazyls have electronic configuration that can originate a FM interaction or not.

Experimental Section

Syntheses. 1,5-Diphenyl-3-(4-R-phenyl)-6-oxo- and -thioxoverdazyl radicals (R = CH$_3$O, CH$_3$, CN, and NO$_2$) were prepared according to a procedure similar to that used by Neugebauer et al.[16] to prepare a 1,3,5-triphenyl-6-oxoverdazyl (TOV) radical. The precursors of the verdazyl radicals (that is, 1,4,5,6-tetrahydro-2,4-diphenyl-6-(4-R-phenyl)-1,2,4,5-tetrazin-3(2*H*)-one and -thione) were also prepared according to a method used by Neugebauer et al.[16]

3-(4-Methoxyphenyl)-1,5-diphenyl-6-oxoverdazyl (*p*-MDpOV). To a stirred solution of 1,4,5,6-tetrahydro-6-(4-methoxyphenyl)-2,4-diphenyl-1,2,4,5-tetrazin-3(2*H*)-one (720 mg, 2 mmol) in dimethyl sulfoxide (20 mL), lead dioxide (4 g) was added and stirring was continued for 2 h. The reaction mixture

* To whom correspondence should be addressed. Tel.: 81-89-927-9588. Fax.: 81-89-927-9590. E-mail: mukai@sci.ehime-u.ac.jp.
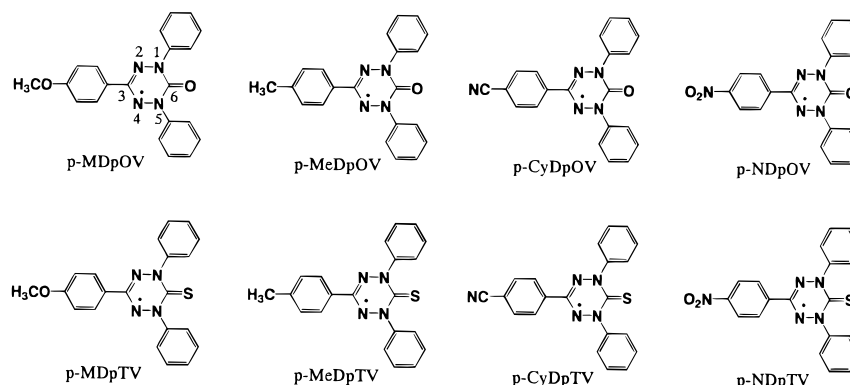† Department of Chemistry.
‡ Department of Physics.

Magnetic Properties of Verdazyl Radical Crystals

J. Phys. Chem. B, Vol. 102, No. 5, 1998 **783**

Figure 1. Molecular structures of 3-(4-R-substituted-phenyl)-1,5-diphenyl-6-oxo- and -thioxoverdazyl radicals.

was filtered. After addition of water and dichloromethane to the filtrate, the organic layer was separated, washed with water, dried (MgSO$_4$), and evaporated under reduced pressure. The residue was chromatographed on silica gel using dichloromethane as eluent. Recrystallization of the residue from ethyl acetate afforded the product as dark-purple thin needle crystals (338 mg, 47%): mp 165–167 °C; UV (dioxane) λ_{max} (log ϵ) 572 (3.14), 420 (2.96 sh), 318 (4.16), 233 (4.88); found: C, 70.81; H, 4.89; N, 15.48%; calcd for C$_{21}$H$_{17}$N$_4$O$_2$: C, 70.58; H, 4.79; N, 15.68%.

The following radicals were prepared similarly.

3-(4-Methylphenyl)-1,5-diphenyl-6-oxoverdazyl (*p*-MeDpOV). Reddish brown powder crystals: mp 208–210 °C; UV (dioxane) λ_{max} (log ϵ): 568 (3.38), 422 (3.10 sh), 318 (4.07), 258 (4.35); found: C, 74.08; H, 5.25; N, 16.41%; calcd for C$_{21}$H$_{17}$N$_4$O: C, 73.88; H, 5.02; N, 16.41%.

3-(4-Cyanophenyl)-1,5-diphenyl-6-oxoverdazyl (*p*-CyDpOV). Reddish brown powder crystals: mp 210–213 °C; UV (dioxane) λ_{max} (log ϵ): 547 (3.19), 429 (3.01), 318 (3.92), 265 (4.35); found: C, 71.69; H, 4.17; N, 19.73%; calcd for C$_{21}$H$_{14}$N$_5$O: C, 71.58; H, 4.00; N, 19.87%.

3-(4-Nitrophenyl)-1,5-diphenyl-6-oxoverdazyl (*p*-NDpOV). Brown powder crystals: mp 179–180 °C; UV (dioxane) λ_{max} (log ϵ): 553 (3.34), 445 (3.28), 317 (4.12), 278 (4.39); found: C, 64.33; H,3.87; N, 18.54%; calcd for C$_{20}$H$_{14}$N$_5$O$_3$: C, 64.51; H, 3.79; N, 18.81%.

3-(4-Methoxyphenyl)-1,5-diphenyl-6-thioxoverdazyl (*p*-MDpTV). Blue-purple powder crystals: mp 165–167 °C; UV (dioxane) λ_{max} (log ϵ): 623 (2.86), 318 (4.59), 253 (4.16); found: C, 67,48; H, 4.68; N, 15.09%; calcd for C$_{21}$H$_{17}$N$_4$OS: C, 67.54; H, 4.59; N, 15.00%.

3-(4-Methylphenyl)-1,5-diphenyl-6-thioxoverdazyl (*p*-MeDpTV). Blue-purple silky needle crystals: mp 167–169 °C; UV (dioxane) λ_{max} (log ϵ): 615 (2.85), 315 (4.52), 247 (4.30); found: C, 70.74; H, 4.78; N, 15.82%; calcd for C$_{21}$H$_{17}$N$_4$S: C, 70.56; H, 4.79; N, 15.67%.

3-(4-Cyanophenyl)-1,5-diphenyl-6-thioxoverdazyl (*p*-CyDpTV). Green silky needle crystals: mp 179–180 °C; UV (dioxane) λ_{max} (log ϵ): 606 (2.82), 325 (4.51), 249 (4.36); found: C, 68.52; H, 3.87; N, 18.86%; calcd for C$_{21}$H$_{14}$N$_5$S: C, 68.46; H, 3.83; N, 19.01%.

3-(4-Nitrophenyl)-1,5-diphenyl-6-thioxoverdazyl (*p*-NDpTV). Green silky needle crystals: mp 181–182 °C; UV (dioxane) λ_{max} (log ϵ): 606 (2.79), 339 (4.42), 260 (4.20 sh); found: C, 61.96; H, 3.66; N, 17.98%; calcd for C$_{20}$H$_{14}$N$_5$O$_2$S: C, 61.84; H, 3.63; N, 18.03%.

Susceptibility Measurement. The paramagnetic susceptibility measurements were carried out with a Shimadzu MB-2 type magnetic torsion balance in the temperature range 77–300 K,

TABLE 1: Magnetic Properties of 3-(4-R-Phenyl)-1,5-diphenyl-6-oxo- and -thioxoverdazyl Radical Crystals

| radical	magnetism	parameters	pascal's diamagnetism (emu/mol)
p-MDpOV	1D AFM Heisenberg linear chain	T_{max} = 17 K $2\,J/k$ = −27.3 K	−0.201 × 10^{-3}
p-MeDpOV	Curie−Weiss	θ = +2.5 K ($2\,J/k$ = +7.0 K)^a	−0.197 × 10^{-3}
p-CyDpOV	1D AFM Heisenberg linear chain	T_{max} = 17 K $2\,J/k$ = −27.3 K	−0.194 × 10^{-3}
p-NDpOV	Curie−Weiss	θ = +1.5 K ($2\,J/k$ = +5.0 K)^a	−0.195 × 10^{-3}
p-MDpTV	1D AFM Heisenberg linear chain	T_{max} = 6.7 K $2\,J/k$ = −10.9 K	−0.218 × 10^{-3}
p-MeDpTV	1D AFM Heisenberg alternating chain	T_{max} = 56 K $2\,J_1/k$ = −92.0 K $2\,J_2/k$ = −64.4 K	−0.213 × 10^{-3}
p-CyDpTV	Curie−Weiss	θ = +2.9 K ($2\,J/k$ = +7.0 K)^a	−0.210 × 10^{-3}
p-NDpTV	Curie−Weiss	θ = −0.9 K	−0.212 × 10^{-3}

^{a} The values of $2\,J/k$ were estimated on the basis of the one-dimensional ferromagnetic Heisenberg model.

and with a SQUID magnetometer (HOXAN HSM-D 2000) in the temperature range 4.2−100 K. The susceptibility at low temperature was measured at 0.02 *T* to avoid saturation effects. The susceptibility of all samples has been corrected for the diamagnetic contribution, calculated by Pascal's method (see Table 1).
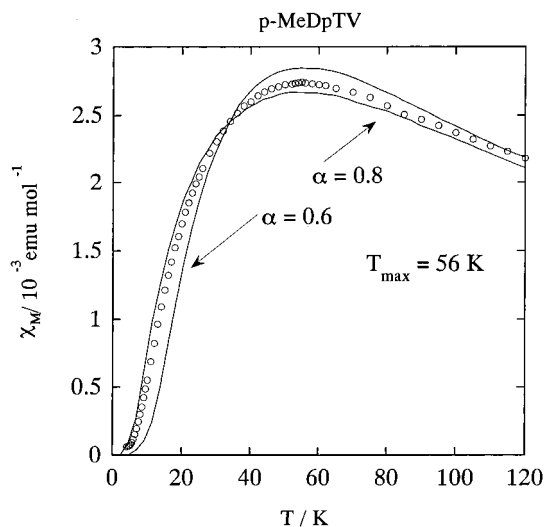
Results

Magnetic Susceptibilities of *p*-MDpOV, *p*-CyDpOV, *p*-MDpTV and *p*-MeDpTV. The magnetic susceptibility, χ_M, obtained for *p*-MDpOV is shown in Figure 2 as a function of temperature. The data have been corrected for the diamagnetic contribution of χ_{dia} = −0.201 × 10^{-3} emu/mol, calculated by Pascal's method. When the temperature is lowered from 300 K, χ_M increases gradually and reaches a broad maximum at T_{max} = 17 ± 1 K. After passing through the maximum, χ_M decreases gradually down to 5 K. Below this temperature, χ_M increases slightly as the temperature is lowered. This increase of the susceptibility at low temperature is probably due to isolated monoradicals that are randomly located in the lattice and/or broken-chain effects.[19]

Similar behavior was observed for the magnetic susceptibilities of *p*-CyDpOV and *p*-MDpTV radicals. The susceptibilities of *p*-CyDpOV and *p*-MDpTV show a broad maximum at 17 ± 1 and 6.7 ± 1 K, respectively, and a small increase in the susceptibility at low temperature that will be attributable to isolated monoradicals.
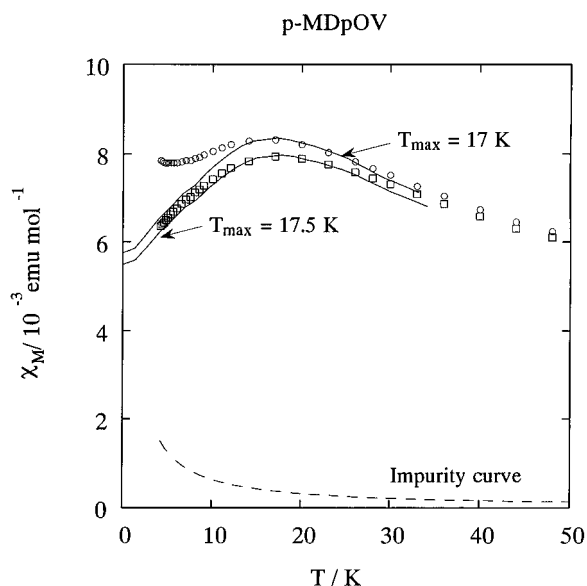
p-MDpOV

Figure 2. Molar magnetic susceptibility (χ_M) of the *p*-MDpOV radical. The open circle (○) curve is the experimental curve. The dashed curve is calculated for 1.7% of a monoradical impurity following the Curie law. The open square (□) curve gives the difference between experimental and impurity curves. The solid curves are the theoretical susceptibilities calculated for the 1D AFM Heisenberg linear chain model with the indicated values of T_{max} = 17.0 and 17.5 K.

p-MeDpTV

Figure 3. Temperature dependence of the molar magnetic susceptibility (χ_M, ○) of *p*-MeDpTV. The solid curves are the theoretical susceptibilities calculated for the 1D AFM Heisenberg alternating chain model (α = 0.6 and 0.8).

The magnetic susceptibility, χ_M, obtained for *p*-MeDpTV radical is shown in Figure 3 as a function of temperature. By lowering the temperature from 300 K, χ_M increases gradually and reaches a broad maximum at T_{max} = 56 ± 1 K. After passing through the maximum, the susceptibility falls off rapidly till 4.2 K. The values of T_{max} obtained are summarized in Table 1.

Magnetic Susceptibilities of *p*-MeDpOV, *p*-NDpOV, *p*-CyDpTV, and *p*-NDpTV. The molar susceptibility, χ_M, of *p*-MeDpOV radical is shown in Figure 4 as a function of the temperature. The susceptibility of *p*-MeDpOV follows the Curie−Weiss law, with a Curie constant of 0.370 emu/mol and a positive Weiss constant (θ) of +2.5 ± 0.2 K in the temperature region 10−300 K. The positive Weiss constant indicates the FM intermolecular interaction of *p*-MeDpOV. A plot of $1/\chi_M$
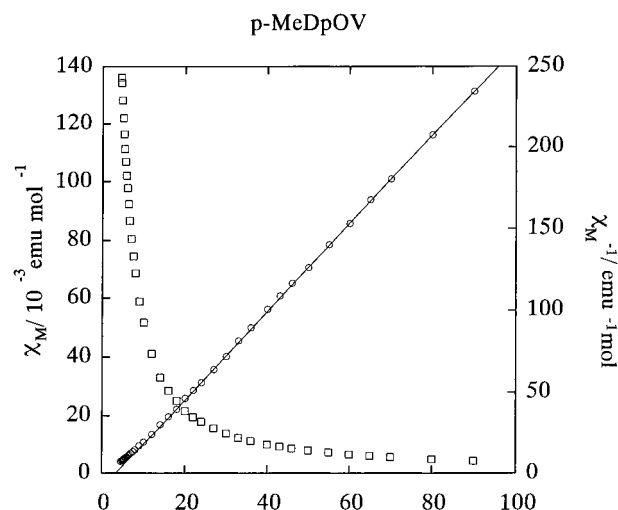
p-MeDpOV

Figure 4. Temperature dependence of the molar magnetic susceptibility (χ_M, □) and inverse magnetic susceptibility ($1/\chi_M$, ○) of *p*-MeDpOV.

against *T* is no longer linear at lower temperature (<10 K; see Figure 4), although a linear extrapolation would still give a positive value of θ. Such a magnetic behavior is characteristic of a FM substance. The radical concentration calculated from the aforementioned Curie constants is 98.3% for *p*-MeDpOV.

Similarly, the magnetic susceptibilities, χ_M, of *p*-NDpOV and *p*-CyDpTV also follow the Curie−Weiss law with Curie constants of 0.376 and 0.366 K emu/mol and positive Weiss constants of θ = +1.5 ± 0.2 and +2.9 ± 0.2 K, respectively, in the temperature region 10−300 K. A plot of $1/\chi_M$ against *T* is no longer linear at lower temperature (<10 K). The radical concentrations, as determined from the susceptibility, are 100% for *p*-NDpOV and 97.4% for *p*-CyDpTV.

On the other hand, the susceptibility of *p*-NDpTV follows the Curie−Weiss law with a Curie constant of 0.374 K emu/mol and a negative Weiss constant of −0.9 ± 0.2 K above 4.2 K. The negative Weiss constant suggests an antiferromagnetic (AFM) intermolecular interaction of *p*-NDpTV. The radical concentration obtained is 99.5% for *p*-NDpTV.

Electronic Structure of 6-Oxoverdazyl Radicals. The orbital energies of five kinds of 6-oxoverdazyl radicals with different substituents (H, OCH_3, CH_3, CN, and NO_2) at the *para*-position of the 3-phenyl ring have been calculated by using an ab initio MO method, to clarify the electronic structure of the verdazyl radicals. Ab initio self-consistent field (SCF) calculations were carried out with the GAUSSIAN 94 program.[20] The basis set used in the present calculations is 3-21G, which has thoroughly been tested on organic molecules and reproduces the experimental results fairly well.[21] The calculation was performed for the molecular structure determined by X-ray analysis of a TOV crystal at room temperature.[16]

The *p*-MO (molecular orbital) energies of the next lowest unoccupied MO (NLUMO), singly occupied MO (SOMO), and the next highest occupied MO (NHOMO) obtained are listed in Table 2. As an example, the *p*-MO energy levels of *p*-MeDpOV radical near the SOMO level are shown in Figure 5, where the α-spin orbitals and the corresponding β-spin orbitals are connected with dotted lines. The most notable feature of this figure is the fact that the NHOMO level of the β-spin (β-NHOMO) is higher than the SOMO of the α-spin (α-SOMO). The exchange interaction within the molecule is great enough to stabilize the α-SOMO energy. This situation is one of the important requirements for the intermolecular FM exchange interaction in organic radical crystals.[22−25]

Magnetic Properties of Verdazyl Radical Crystals

J. Phys. Chem. B, Vol. 102, No. 5, 1998 **785**
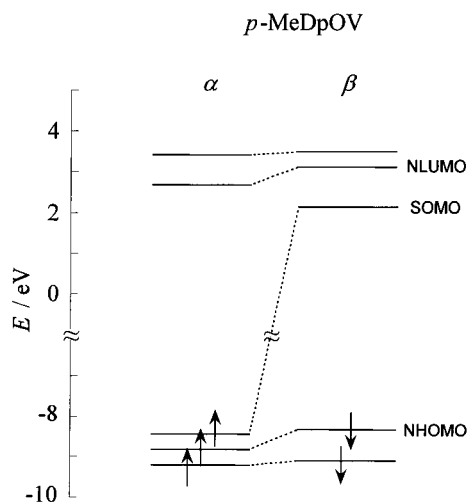
p-MeDpOV

Figure 5. Orbital energies of *p*-MeDpOV radical. Only the *p*-MO levels close to SOMO are shown.

TABLE 2: p-MO Energy Levels of the NLUMO, SOMO, and NHOMO with the α- and β-Spin of 3-(4-R-phenyl)-1,5-diphenyl-6-oxoverdazyl Radical Molecules

radical	orbital	α spin, E (eV)	β spin, E (eV)
TOV	NLUMO	2.52	3.03
	SOMO	−8.48	2.10
	NHOMO	−8.88	−8.51
p-MDpOV	NLUMO	2.69	3.11
	SOMO	−8.49	2.10
	NHOMO	−8.84	−8.28
p-MeDpOV	NLUMO	2.68	3.13
	SOMO	−8.44	2.15
	NHOMO	−8.82	−8.33
p-CyDpOV	NLUMO	2.84	2.73
	SOMO	−8.65	2.10
	NHOMO	−9.06	−8.92
p-NDpOV	NLUMO	2.07	2.53
	SOMO	−8.61	1.94
	NHOMO	−9.00	−8.60

Discussion

Generally, the organic free radicals have a *g*-value very close to that of the free electron ($g = 2.0023$). In fact, the *g*-value of TOV determined by an electron spin resonance (ESR) measurement is 2.0037 in toluene at room temperature.[16] From this fact we can presume a small spin−orbit interaction and consequently an isotropic exchange interaction for 3-(4-R-phenyl)-1,5-diphenyl-6-oxo- and -thioxoverdazyl radicals. Thus, the $S = 1/2$ isotropic Heisenberg model is most suitable for describing the present system.

The measured susceptibilities of *p*-MDpOV, *p*-CyDpOV, *p*-MDpTV, and *p*-MeDpTV were compared with theoretical predictions based on Heisenberg exchange-coupled alternating linear chains.[19,26] The corresponding spin Hamiltonian is given by

$$H = -2J_1 \sum_{i=1}^{N/2} S_{2i} S_{2i+1} - 2J_2 \sum_{i=1}^{N/2} S_{2i-1} S_{2i} \qquad (1)$$

where J_1 and J_2 are the nearest-neighbor exchange integrals. Negative values of J_1 and J_2 corresponding to AFM coupling are appropriate for the free radicals considered here. The α($= J_2/J_1$) parameter conveniently indicates the degree of alternation and α = 1 corresponds to the uniform limit, that is, a nonalternating AFM chain. When α = 0, corresponding to an isolated dimer (spin-pair) system, the susceptibility should be interpreted by the singlet−triplet equilibrium model.

The measured susceptibility of *p*-MDpOV with $T_{max} = 17$ K was compared with theoretical values calculated for 1D AFM Heisenberg linear chain model (α = 1).[19,26] As shown in Figure 2, the susceptibility−temperature data (open circle) for *p*-MDpOV deviate from theoretical values (solid curve) at low temperature below T_{max} because of the existence of impurity radicals (1.7%). When the low-temperature paramagnetic impurity curve (dashed curve) is subtracted from the experimental one, the corrected susceptibility (open square) shown in Figure 2 is obtained. This susceptibility can be well explained by a theoretical curve calculated for the 1D AFM Heisenberg linear chain model (α = 1) with the value of $T_{max} = 17.5$ K. The exchange integral (2 *J/k*) was estimated to be −27.3 K, using the relation $kT_{max}/|J| = 1.282$.

Similarly, the magnetic susceptibilities of *p*-CyDpOV and *p*-MDpTV were interpreted in terms of a nonalternating AFM Heisenberg linear chain model (α = 1). The values of 2 *J/k* obtained are summarized in Table 1.

The measured susceptibility of *p*-MeDpTV with $T_{max} = 56$ K was compared with theoretical values calculated for the 1D AFM Heisenberg alternating chain model.[26] As shown in Figure 3, the susceptibility can be well explained by a 1D AFM Heisenberg alternating chain model with an exchange interaction of 2 $J_1/k = -92.0$ K (alternation parameter α = J_2/J_1 = 0.7).

Recently, we studied the magnetic properties of 1,5-dimethyl- and 1,5-diphenyl-6-oxo- and -thioxoverdazyl radical crystals.[11−14,18,27] These verdazyl radicals are aromatic compounds with a delocalized *p*-electron system and planar molecular structure,[16] and generally show magnetic properties that can be explained by a 1D AFM Hisenberg linear chain model. On the other hand, two of these verdazyls, that is, 3-(4-chlorophenyl)-1,5-dimethy-6-thioxoverdazyl (*p*-CDTV) and 3-(4-chlorophenyl)-1,5-diphenyl-6-oxoverdazyl (*p*-CDpOV), have been found to be a new and bulk ferromagnet with the Curie temperature of $T_c = 0.68$ K and $T_c = 0.21$ K, respectively. Furthermore, these radicals behave as quasi-1D Heisenberg ferromagnets with intra- and interchain exchange interactions (*J* and *zJ′*) of 2 *J/k* = +12.0 K and *zJ′/k* = 0.21 K, and 2 *J/k* = +11.0 K and *zJ′/k* = 0.03 K above T_c, respectively.[11−14,28] *p*-CDpOV has higher one-dimensionality than *p*-CDTV.

As described in a previous section, the susceptibilities of *p*-MeDpOV, *p*-NDpOV, and *p*-CyDpTV follow the Curie−Weiss law, with positive Weiss constant of +2.5, +1.5, and +2.9 K, respectively, in the temperature region 10−300 K. A plot of $1/\chi_M$ against *T* is no longer linear at low temperature (<10 K). Therefore, the low-temperature behavior of the susceptibility, χ_M, of these radical crystals was tentatively analyzed on the basis of the quasi-1D FM Heisenberg model.

In such a case, the susceptibility of a 1D ferromagnet with $S = 1/2$, χ_{1D}, is given by eq 2:

$$\chi_{1D} = \frac{Ng^2\mu_B^2}{4kT}\left\{1 + \left(\frac{J}{kT}\right)^\alpha\right\} \qquad (2)$$

with α = 1 for *kT/J* > 1.[19] For lower temperatures (*kT/J* < 1), however, *a* depends on *T* (*a* → 4/5 for *T* → 0). In fact, above 4.2 K, the susceptibilities of *p*-MeDpOV are well reproduced by eq 2 with 2 *J/k* = +7.0 ± 1.0 K and *g* = 2.00, as shown in Figure 6. Similarly, the values of the exchange interaction for *p*-NDpOV and *p*-CyDpTV were estimated to be 2 *J/k* = +5.0 ± 1.0 K and +7.0 ± 1.0 K, respectively.

A 1D magnet with localized spins is one of the simplest systems of many-body problems from which exact or correct physical quantities have been derived. For 1D Heisenberg
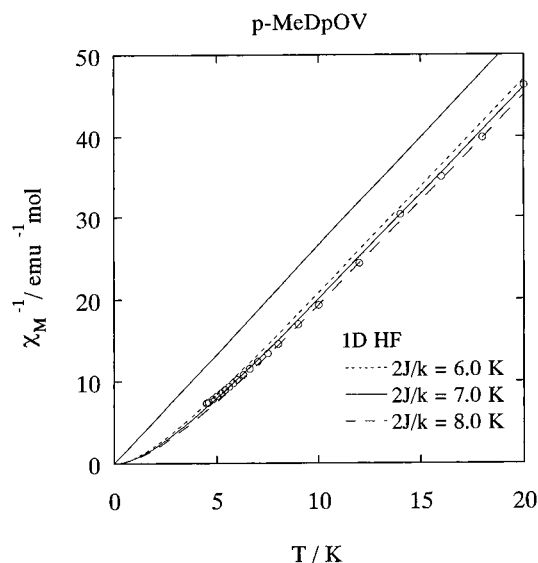
Figure 6. Inverse magnetic susceptibility ($1/\chi_M$) of *p*-MeDpOV at low temperatures. Above 4.2 K, the observed values (open circles) obey the theoretical results for the 1D isotropic Heisenberg ferromagnet (HF) with $2 J/k = +7.0 \pm 1.0$ K.[20] The straight line corresponds to χ_M of the paramagnet with $g = 2.00$ and $S = 1/2$.

antiferromagnets with $S = 1/2$, the physical properties theoretically expected of these antiferromagnets have been experimentally checked with abundant real magnetic compounds. The magnetic properties of *p*-MDpOV, *p*-CyDpOV, and *p*-MDpTV studied in the present work belong to this group and can be explained by the 1D AFM Heisenberg linear chain model.

However, for 1D FM systems the situation differs from the case of antiferromagnets, because we can rarely get the 1D quantum FM substances. Consequently, only a few examples of a 1D Heisenberg ferromagnet, such as $(C_6H_{11}NH_3)CuCl_3$,[29] $K_2Cu_{0.59}Zn_{0.41}F_4$,[30] and the γ-phase of *p*-NPNN,[3] have been reported. *p*-CDTV and *p*-CDpOV radicals belong to this group, as already described. Furthermore, surprisingly, three of eight verdazyls studied exhibit an intermolecular FM interaction, and behave as a quasi-1D ferromagnet. It will be necessary to discuss the origin of such a FM interaction observed for the aforementioned verdazyl radical crystals.

Awaga et al.[22,23] studied the electronic structure of galvinoxyl radical, and found that α-SOMO and α-NLUMO (NLUMO: the lowest unoccupied MO) of galvinoxyl are so stabilized that the energies of α-SOMO and α-NLUMO come close to those of β-NHOMO (NHOMO: the highest doubly occupied MO) and β-SOMO, respectively. In the case of α-SOMO and β-NHOMO, the orbital energy of α-SOMO becomes even lower than that of β-NHOMO; this result implies that the electron in β-NHOMO is more easily transferred in the charge transfer (CT) interaction than that in α-SOMO, leaving the triplet state behind. They reported that this situation is one of the important conditions for the intermolecular FM exchange interaction in galvinoxyl radical crystals. Furthermore, similar studies have been obtained for *p*-NPNN radicals.[24,25]

In the present work, ab initio MO calculations were carried out for five kinds of 6-oxoverdazyl radicals. As listed in Table 2, the energy level of β-NHOMO is higher than that of α-SOMO in *p*-MDpOV and *p*-MeDpOV radicals, and the energy level of β-NHOMO is close to that of α-SOMO in TOV and *p*-NDpOV. The result indicates that in these verdazyl radicals, the exchange interaction within the molecule is great enough to stabilize the α-SOMO. In other words, the spin correlation causes a large spin polarization effect in 6-oxoverdazyl radicals. This feature

closely resembles that in the FM organic radical, galvinoxyl, and β-*p*-NPNN radicals.[22-25] Thus, the FM interaction of the verdazyl radicals is considered to originate mainly from the β-SOMO-β-NHOMO charge-transfer interaction.

As already described, an intermolecular FM interaction was observed for *p*-MeDpOV and *p*-NDpOV radicals. On the other hand, TOV, *p*-MDpOV, and *p*-CyDpOV show AFM interactions, although the electronic structure of the verdazyls except for *p*-CyDpOV satisfies one of the important conditions for the intermolecular FM exchange interaction in organic radical crystals, proposed by Awaga et al.[22-25] To discuss the details of the origin of intermolecular FM interaction observed for verdazyl radicals, information about the crystal structures of the verdazyl radicals are necessary. However, to our regret, we have not succeeded in obtaining single crystals suitable for X-ray structure analyses to date.

References and Notes

(1) Kinoshita, M.; Turek, P.; Tamura, M.; Nozawa, K.; Shiomi, D.; Nakazawa, Y.; Ishikawa, M.; Takahashi, M.; Awaga, K.; Inabe, T.; Maruyama, Y. *Chem. Lett.* **1991**, 1225.

(2) Tamura, M.; Nakazawa, Y.; Shiomi, D.; Nozawa, K.; Hosokoshi, Y.; Ishikawa, M.; Takahashi, M.; Kinoshita, M. *Chem. Phys. Lett.* **1991**, *186*, 401.

(3) Nakazawa, Y.; Tamura, M.; Shirakawa, N.; Shiomi, D.; Takahashi, M.; Kinoshita, M.; Ishikawa, M. *Phys. Rev.* **1992**, *B46*, 8906.

(4) Chiarelli, R.; Rassat, A.; Rey, P. *J. Chem. Soc. Chem. Commun.* **1992**, 1081.

(5) Chiarelli, R.; Novak, M. A.; Rassat, R.; Tholence, J. L. *Nature* **1993**, *363*, 147.

(6) Nogami, T.; Tomioka, K.; Ishida, T.; Yoshikawa, H.; Yasui, M.; Iwasaki, F.; Iwamura, H.; Takeda, N.; Ishikawa, M. *Chem. Lett.* **1994**, 29.

(7) Nogami, T.; Ishida, T.; Yasui, M.; Iwasaki, F.; Takeda, N.; Ishikawa, M.; Kawasaki, T.; Yamaguchi, K. *Bull. Chem. Soc. Jpn.* **1996**, *69*, 1841, and references cited therein.

(8) Sugawara, T.; Matsushita, M. M.; Izuoka, A.; Wada, N.; Takeda, N.; Ishikawa, M. *J. Chem. Soc., Chem. Commun.* **1994**, 1723.

(9) Cirujeda, J.; Mas, M.; Molins, E.; de Panthou, F. L.; Laugier, J.; Park, J. G.; Paulsen, C.; Rey, P.;. Rovira, C.; Veciana, J. *J. Chem. Soc., Chem. Commun.* **1995**, 709.

(10) Caneschi, A.; Ferraro, F.; Gatteschi, D.; Lirzin, A.; Novak, M. A.; Rentschler, E.; Sessoli, R. *Adv. Mater.* **1995**, *7*, 476.

(11) Mukai, K.; Konishi, K.; Nedachi, K.; Takeda, K. *J. Magn. Magn. Mater.* **1995**, *140–144*, 1449.

(12) Mukai, K.; Nedachi, K.; Takiguchi, M.; Kobayashi, T.; Amaya, K. *Chem. Phys. Lett.* **1995**, *238*, 61.

(13) Mukai, K.; Konishi, K.; Nedachi, K.; Takeda, K. *J. Phys. Chem.* **1996**, *100*, 9658.

(14) Takeda, K.; Hamano, T.; Kawae, T.; Hidaka, M.; Takahashi, M.; Kawasaki, S.; Mukai, K. *J. Phys. Soc. Jpn.* **1995**, *64*, 2343.

(15) Sugimoto, T.; Tsuji, M.; Suga, T.; Hosoito, N.; Ishikawa, M.; Takeda, N.; Shiro, M. *Mol. Cryst. Liq. Cryst. Sci. Technol., Sect. A* **1995**, *272*, 183.

(16) Neugebauer, F. A.; Fischer, H.; Krieger, C. *J. Chem. Soc., Perkin Trans. 2*, **1993**, 535.

(17) Kremer, R. K.; Kanellakopulos, B.; Bele, P.; Brunner, H.; Neugebauer, F. A. *Chem. Phys. Lett.* **1994**, *230*, 255.

(18) Mukai, K.; Kawasaki, S.; Jamali, J. B.; Achiwa, N. *Chem. Phys. Lett.* **1995**, *241*, 618.

(19) Bonner, J. C.; Fisher, M. E. *Phys. Rev.* **1964**, *A135*, 640.

(20) Frisch, M. J.; Trucks, G. W.; Schlegel, H. B.; Gill, P. M. W.; Johnson, B. G.; Robb, M. A.; Cheeseman, J. R.; Keith, T.; Petersson, G. A.; Montgomery, J. A.; Raghavachari, K.; Al-Laham, M. A.; Zakrzewski, V. G.; Ortiz, J. V.; Foresman, J. B.; Cioslowski, J.; Stefanov, B. B.; Nanayakkara, A.; Challacombe, M.; Peng, C. Y.; Ayala, P. Y.; Chen, W.; Wong, M. W.; Andres, J. L.; Replogle, E. S.; Gomperts, R.; Martin, R. L.;

Magnetic Properties of Verdazyl Radical Crystals

J. Phys. Chem. B, Vol. 102, No. 5, 1998 **787**

Fox, D. J.; Binkley, J. S.; Defrees, D. J.; Baker, J.; Stewart, J. P.; Head-Gordon, M.; Gonzalez, C.; Pople, J. A. *Gaussian 94*; Gaussian: Pittsburgh, PA, 1995.

(21) Hehre, W. J.; Radom, L.; Schleyer, P. v. R.; Pople, J. A. *Ab Initio Molecular Orbital Theory*; Wiley: New York, 1986.

(22) Awaga, K.; Sugano, T.; Kinoshita, M. *Chem. Phys. Lett.* **1987**, *141*, 540.

(23) Awaga, K.; Maruyama, Y. *J. Chem. Phys.* **1989**, *91*, 2743.

(24) Awaga, K.; Inabe, T.; Nagashima, U.; Maruyama, Y. *J. Chem. Soc., Chem. Commun.* **1989**, 1617.

(25) Kinoshita, M. *Jpn. J. Appl. Phys.* **1994**, *33*, 5718.

(26) Bonner, J. C.; Blote, H. W. J.; Bray, J. W.; Jacobs, I. S. *J. Appl. Phys.* **1979**, *50*, 1810.

(27) Mukai, K.; Wada, N.; Jamali, J. B.; Achiwa, N.; Narumi, Y.; Kindo, K.; Kobayashi, T.; Amaya, K. *Chem. Phys. Lett.* **1996**, *257*, 538.

(28) Takeda, K.; Konishi, K.; Nedachi, K.; Mukai, K. *Phys. Rev. Lett.* **1995**, *74*, 1673.

(29) Haines, D. N.; Drumheller, J. E. *Phys. Rev. Lett.* **1987**, *58*, 2702.

(30) Takeda, K.; Okuda, Y.; Yamada, I.; Haseda, T. *J. Phys. Soc. Jpn.* **1981**, *50*, 1917.